

Article

# The Preparation of TiO<sub>2</sub> Film by the Sol-Gel Method and Evaluation of Its Self-Cleaning Property

Yu Liang <sup>1,2</sup> , Sijia Sun <sup>1</sup>, Tongrong Deng <sup>1</sup>, Hao Ding <sup>1,\*</sup>, Wanting Chen <sup>1</sup> and Ying Chen <sup>1</sup>

<sup>1</sup> Beijing Key Laboratory of Materials Utilization of Nonmetallic Minerals and Solid Wastes, National Laboratory of Mineral Materials, School of Materials Science and Technology, China University of Geosciences (Beijing), Beijing 100083, China; liangyuaadd@126.com or liangyuaadd@gmail.com (Y.L.); ssjcugb@163.com (S.S.); 18010157480@163.com (T.D.); wantingchen123@163.com (W.C.); yingchen1827@163.com (Y.C.)

<sup>2</sup> School of Materials Science and Technology, Shenyang University of Chemical Technology, Shenyang 110142, China

\* Correspondence: dinghao@cugb.edu.cn or dinghao113@126.com

Received: 5 December 2017; Accepted: 12 March 2018; Published: 19 March 2018

**Abstract:** TiO<sub>2</sub> sol was produced by the sol-gel method through the hydrolysis and the aging of tetrabutyl titanate and the TiO<sub>2</sub> film was obtained by dipping and uniform lifting of the acid-treated and ultrasound-treated clean glass slides into the TiO<sub>2</sub> sol followed by aging, drying, and calcination. The effect of the hydrolysis control agents to the formed sol was researched and the crystalline state, the morphology, and the photocatalytic properties of the products after calcination were characterized. The structural morphology, the contact angles before and after illumination, and the self-cleaning properties of the TiO<sub>2</sub> film were characterized as well. The results showed that by using acetylacetone as the hydrolysis control agent, the formed TiO<sub>2</sub> sol had relatively high stability. The product after the calcination of the TiO<sub>2</sub> sol was of single anatase type with crystalline size of 18–20 nm and it could degrade nearly 100% of methylene blue after 90 min illumination. The formed TiO<sub>2</sub> film is compact, continuous, smooth, and had the properties of super-hydrophilicity (after 30 min illumination due to its contact angle decreasing from 21° to nearly 0°) and anti-fogging capability, which indicated its excellent self-cleaning property.

**Keywords:** sol-gel method; TiO<sub>2</sub> film; hydrolysis control agent; anti-fogging property; self-cleaning property

## 1. Introduction

Titanium dioxide is a kind of material that is mostly used as white pigments for its outstanding properties, such as high whiteness, brightness, non-toxicity, and strong hiding power [1]. It is also well known for its excellent chemical stability, biological nontoxicity, and low cost [2–4]. It has been used extensively as a photocatalyst since 1971, when articles published by Formenti et al. [5] and K. Honda [6] caused a global upsurge of the extensive use of TiO<sub>2</sub> as a photocatalyst. Since this decade, a number of processes, such as effluent detoxification and disinfection, water splitting, and organic synthesis, have used nano-TiO<sub>2</sub> as photocatalysis [7–12]. A large amount of TiO<sub>2</sub> has been used in Asia, especially in China, South Korea, and Japan [13–15]. The self-cleaning effect of TiO<sub>2</sub> under ultraviolet (UV) irradiation due to the photoinduced hydrophilic properties of TiO<sub>2</sub> is also a feature [16,17]. Clear and unified explanations have been made regarding the mechanisms of the TiO<sub>2</sub> photocatalysis process. A series of reactions have been induced by the photogenerated e<sup>-</sup> (electrons) and h<sup>+</sup> (holes) from the photoexcited catalyst in the system. O<sub>2</sub><sup>-</sup> and subsequent H<sub>2</sub>O<sub>2</sub> and OH• radicals [18,19] were produced as a result of these different photoreactions and then facilitated the

decomposition of the organic substances [20,21]. Two effects lead to the self-cleaning property of nano-TiO<sub>2</sub> [22,23]. One is that the active components induced by the photocatalytic action of TiO<sub>2</sub> can react with the pollutants adhering to the surface, thus achieving the decomposition of pollutants. The other is that the decomposed products can be washed away by rain, which maintains the cleanness of the material surface [24]. Kim et al. [23] synthesized a layer of water-resistant and surface-coatable C-PEG (poly(ethyleneglycol)-g-[poly(dimethylaminomethacrylate)]) with TiO<sub>2</sub> nanoarticles (NPs) on a glass surface via catechol chemistry and they found that the final product gained self-cleaning capabilities owing to the hydrophilic nature imparted to the surface by controlling the amounts of catechol moiety and TiO<sub>2</sub> NPs on the polymer. Lucas et al. [25] combined phase change materials (PCM) microcapsules and TiO<sub>2</sub> nanoparticles together and found it made mortars with multiple functionalities including self-cleaning properties. Zhang et al. [26] produced a nano-TiO<sub>2</sub> polyacrylate hybrid dispersion and successfully fixed it on cotton fabric. The final product was proved to have good self-cleaning properties by decomposing the red wine besmirch on it under natural light.

Various ways have been developed to synthesize nano-sized TiO<sub>2</sub> particles or TiO<sub>2</sub> film. Among them, the most important methods of producing titanium dioxide are the hydrolysis and calcination of titanium sulfate and the oxidation of titanium tetrachloride [27]. Other synthesis methods are precipitation of titanium hydroxide, pyrolysis of the titanium citrate precursor [28], and hydrolysis of TiCl<sub>4</sub>. The sol-gel method was first reported in 1939 by Geffcken and Berger and has received great attention since then. It has become a commonly used method for producing TiO<sub>2</sub> due to its simple operation, low reaction temperature, good chemical homogeneity, low requirements for the substrates, and high purity of the product. However, some factors have restricted the scope of applications of nano-TiO<sub>2</sub>. TiO<sub>2</sub> nanoparticles tend to form serious agglomerations, which of course increase the apparent grain size to the micron scale and inhibit its performance, including the self-cleaning effect. The recovery of nano-TiO<sub>2</sub> particles is also a problem. It is hard to recover nano-TiO<sub>2</sub> powder from water, thus forming secondary pollution. The residual nano-TiO<sub>2</sub> particles can restrain the growth and reproduction of cells, produce free radicals, and harm DNA [29,30]. In order to solve the problem of recycling TiO<sub>2</sub>, it is beneficial to produce TiO<sub>2</sub> film instead of producing TiO<sub>2</sub> nanoparticles. Barbana et al. [31] produced TiO<sub>2</sub> film using the technique of pulsed electrophoretic deposition on the surface of stainless steel and found that the TiO<sub>2</sub> film exhibited good photocatalytic activity due to its crystalline size and the synergetic effect of Fe<sub>2</sub>O<sub>3</sub>. However, there are few articles talking about the effects of the main parameters and their optimization during the preparation process of TiO<sub>2</sub> film. Among them, TiO<sub>2</sub> sol is the precursor of TiO<sub>2</sub> film and has extremely important impacts on the formed film. On the one hand, the stability of the sol has an extremely important role in the uniformity of the formed TiO<sub>2</sub> film. Only transparent and precipitation-free sol can be used to produce TiO<sub>2</sub> film successfully. On the other hand, the crystalline phase of the sol after calcination should be in single anatase phase or in anatase phase with a slight amount of rutile phase with its crystal size in the nano-scale, thus leading to good photocatalytic degradation ability and light-induced hydrophilic effect of the formed TiO<sub>2</sub> thin film.

In this article, the TiO<sub>2</sub> sol and TiO<sub>2</sub> film were produced by the hydrolysis of tetrabutyl titanate under three different hydrolysis control agents by the sol-gel method. The effects of the hydrolysis control agents, the structures of the particles after the calcination of the sol, and the self-cleaning properties of the TiO<sub>2</sub> film were investigated and evaluated.

## 2. Materials and Methods

### 2.1. Materials

Tetrabutyl titanate was obtained from TCI company in Shanghai (China). Acetylacetone and acetic acid were purchased from Xilong Chemical Co., Ltd. in Guangdong Province (Dongguan, China). Anhydrous ethanol, triethanolamine, hydrochloric acid, and methylene blue were obtained

from Beijing Chemical Plants in Beijing (China). They were all analytical agents. All chemicals were used as received without further purification.

## 2.2. Preparation of TiO<sub>2</sub> Powder and TiO<sub>2</sub> Thin Film

Tetrabutyl titanate and the hydrolysis control agent were dissolved in anhydrous ethanol separately and stirred adequately. Then, the hydrolysis control agent solution was added into the tetrabutyl titanate solution and stirred adequately. The mixed solution of water and anhydrous ethanol were added to the former mixed solution drop by drop with magnetic stirrer stirring for 12 h in room temperature, forming TiO<sub>2</sub> sol. The mole ratio of tetrabutyl titanate to hydrolysis control agent to water was 1:0.5:2. The TiO<sub>2</sub> powder was obtained by aging treatment, drying (at 60 °C), and calcination of TiO<sub>2</sub> sol. The TiO<sub>2</sub> thin film was obtained by dipping and uniformly lifting the acid-treated and ultrasound-treated clean glass slides into the TiO<sub>2</sub> sol followed by aging, drying, and calcination.

## 2.3. Characterization

The X-ray diffraction patterns were obtained on a Rigaku Rotaflex X-ray powder diffractometer (Rigaku, Tokyo, Japan), employing Cu K $\alpha$  radiation, 40 kV, 100 mA. The X-ray diffraction (XRD) patterns in the 2 $\theta$  range from 3° to 70° were collected at 4°/min. The contact angle was measured by Rame-Hart 200-F1 goniometer (Rame-hurt, Succasunna, NJ, USA) using deionized water as the media. The UV-vis diffuse reflectance spectra were tested with a spectrophotometer (Cary 5000, Varian, Palo Alto, CA, USA). The microstructure and morphologies were investigated by scanning electron microscopy (SEM; S-3500N, Hitachi, Tokyo, Japan) and transmission electron microscopy (TEM; JEOL JEM-2010, JEOL, Tokyo, Japan). The photocatalytic activities were evaluated by the decomposition of methylene blue under UV light illumination ( $\lambda < 420$  nm). In a typical photocatalytic experiment, 50 mg samples were dispersed in 50 mL methylene blue solution (with its concentration 10 ppm) in a photochemical reactor (BL-GHX-V, Shanghai, China). Prior to illumination, the suspension was magnetically stirred in the dark for 1 h to achieve the adsorption–desorption equilibrium on the surface of the photocatalyst. Light illumination was conducted using a 300 W mercury lamp as the UV light resonance. During the photodecomposition process, samples were withdrawn at regular intervals and centrifuged to remove the photocatalyst for analysis. The filtrate was then analyzed using a UV-vis spectrophotometer to measure the absorption of methylene blue in the range of 200–800 nm. The self-cleaning property of the TiO<sub>2</sub> film was tested by dropping methylene blue on the surfaces with or without TiO<sub>2</sub> film. When the liquid dried, these surfaces were illuminated under UV light for 30 min and washed slowly with water. The self-cleaning property of the film was judged by the relative area of the remaining methylene blue. The antifogging property of TiO<sub>2</sub> film was judged by illuminating the surfaces with or without TiO<sub>2</sub> film for 30 min under UV light, then water was sprayed on the surfaces to see how many water droplets emerged on the surfaces.

## 3. Results and Discussion

### 3.1. The Effects of Different Hydrolysis Agents on the Stability and Crystalline Phase of TiO<sub>2</sub> Sol

#### 3.1.1. The Stability of TiO<sub>2</sub> Sol

Three different hydrolysis control agents (acetylacetone, triethanolamine, acetic acid, and hydrochloric acid mixture (2.5:1, volume ratio)) were used in this study to prepare TiO<sub>2</sub> sol. The mole ratio of tetrabutyl titanate to hydrolysis control agent to water was 1:0.5:2. The colors of the formed sol were observed and recorded (Table 1) (The sol is transparent, if not clearly mentioned “there is precipitation”). When the hydrolysis control agents added were acetylacetone and the mixture of acetic acid and hydrochloric acid, respectively, the color and status of the TiO<sub>2</sub> sol can be maintained as long as 48 h, meaning good stability of the sol. However, when the hydrolysis control agent was

triethanolamine, the sol was not that stable and formed some precipitation when the aging time was 48 h.

**Table 1.** The color and status of TiO<sub>2</sub> sol with different aging times.

Hydrolysis Control Agent	0 h	6 h	18 h	48 h
acetylacetone	Brown	Brown	Brown	Brown
triethanolamine	Colorless	Pale white	Pale white	Some precipitation
acetic acid and hydrochloric acid mixture	Light brown	Light brown	Light brown	Light brown

### 3.1.2. The Crystalline Phase of TiO<sub>2</sub> after Calcination of the Sol

XRD patterns of the products obtained by the calcination of the sol in different hydrolysis control agents and aging times are shown in Figure 1. Anatase TiO<sub>2</sub> formed after calcination of the sol at 500 °C by all three hydrolysis control agents with some rutile TiO<sub>2</sub> formed, together marked as R.

When the hydrolysis control agent was triethanolamine, rutile TiO<sub>2</sub> powder formed together with anatase TiO<sub>2</sub>. Compared with others, the intensity of the characteristic peaks of the rutile TiO<sub>2</sub> was the largest when the aging time was 0 h, corresponding to the highest amount of rutile TiO<sub>2</sub>. The amount of rutile phase decreased but still existed as the aging time was between 6 h and 48 h. Rutile phase TiO<sub>2</sub> only existed in the product when using acetylacetone as the hydrolysis control agent and the aging time is 0 h. When the hydrolysis control agent was the mixture of acetic acid and hydrochloric acid, the formed TiO<sub>2</sub> powder was in a single anatase type and did not change as the aging time increased.

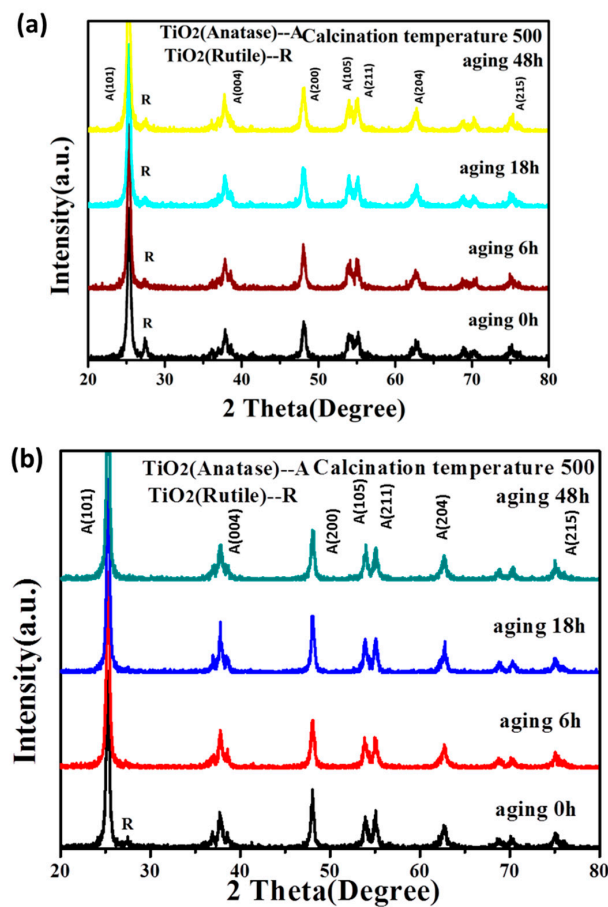
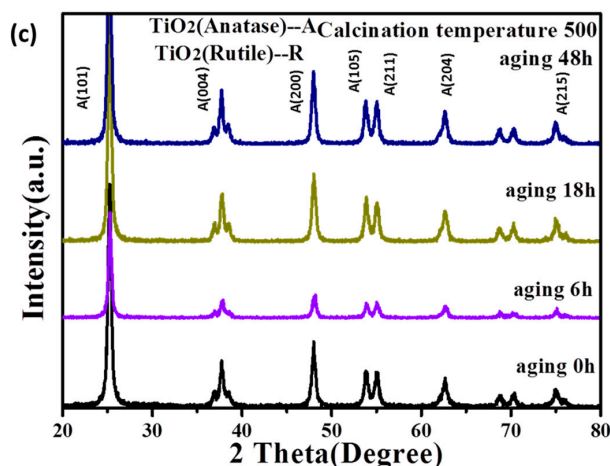


Figure 1. Cont.



**Figure 1.** The XRD patterns of TiO<sub>2</sub> powder formed by the calcination of the sol using different hydrolysis control agents with different aging time. The hydrolysis control agents were: (a) triethanolamine; (b) acetylacetone; (c) the mixture of acetic acid and hydrochloric acid. The calcination temperature was 500 °C.

Moreover, the crystal size of TiO<sub>2</sub> at (101) was calculated by the Debye–Scherrer equation:

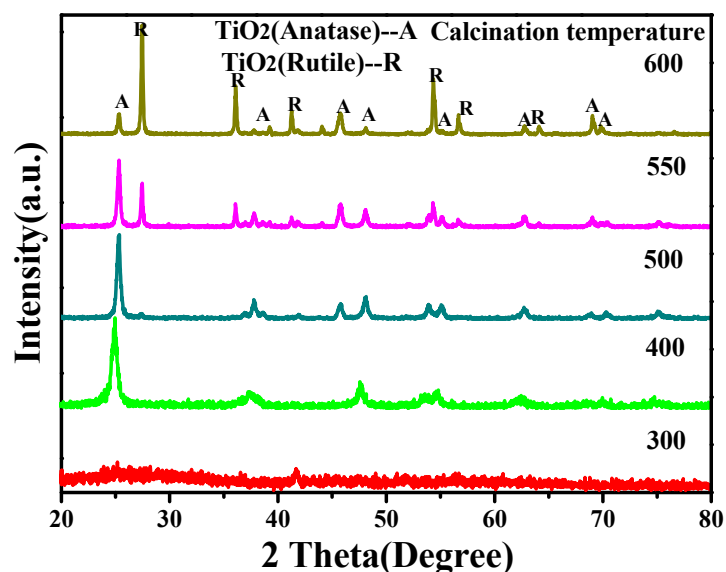
$$D_{hkl} = \frac{k\lambda}{\beta \cos \theta} \quad (1)$$

where  $D_{hkl}$  is the average crystal size at (hkl) crystal plane;  $k$  is the form factor, which is close to 1;  $\beta$  is full width at half maximum (FWHM);  $\lambda$  is the wavelength of the x-ray;  $\theta$  is the diffraction angle. The results showed that the anatase crystal size of TiO<sub>2</sub> was 20–21 nm, 16–17 nm, and 18–19 nm when using acetylacetone, triethanolamine, and the mixture of acetic acid and hydrochloric acid as hydrolysis control agent, respectively. The crystal size of TiO<sub>2</sub> after calcination was kept at a relatively small scale and was not affected by aging time.

Based on the above experimental results, it can be concluded that acetylacetone is the most suitable hydrolysis control agent for the formation of TiO<sub>2</sub> sol. Triethanolamine is not that suitable, based on the facts that the sol formed was not stable and the crystalline type of the final products is not pure anatase type TiO<sub>2</sub>, but a mixture of rutile and anatase type TiO<sub>2</sub>. Considering the environmental effect, the mixture of acetic acid and hydrochloric acid is not as suitable as acetylacetone.

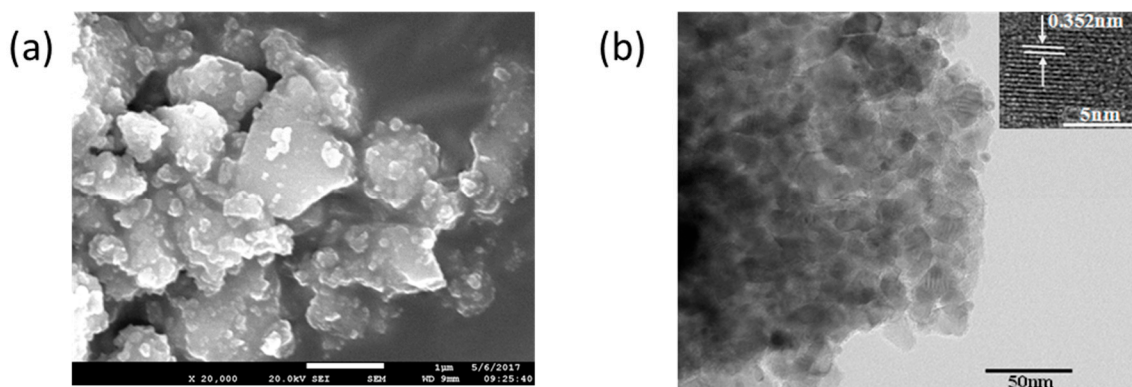
### 3.2. The Effect of Calcination Temperature to the Crystalline Phase and Morphology of TiO<sub>2</sub>

Figure 2 shows the XRD patterns of the samples obtained after TiO<sub>2</sub> sol being calcined at different temperatures. When the calcination temperature was 300 °C, there was no obvious crystal formation, except for the broad scattering peak when  $2\theta$  was 25°. As the temperature increased to 400–500 °C, the diffraction peak of anatase TiO<sub>2</sub> emerged with a slight amount of rutile TiO<sub>2</sub>. The higher the temperature, the sharper the peak shape. When the temperature increased to 550 °C, the final product was a mixture of anatase TiO<sub>2</sub> and rutile TiO<sub>2</sub>. The diffraction peak intensity of rutile TiO<sub>2</sub> increased further when the temperature reached 600 °C, which is in accordance with the literature [32]. Meanwhile, the peak intensity of anatase TiO<sub>2</sub> decreased to a relatively low level. Since anatase TiO<sub>2</sub> has much better photocatalytic properties than rutile TiO<sub>2</sub>, the proper temperature is 500 °C.



**Figure 2.** The XRD patterns of  $\text{TiO}_2$  powder after being calcined at 300 °C, 400 °C, 500 °C, 550 °C, and 600 °C. The hydrolysis agent was acetylacetone and the aging time was 6 h.

From the SEM images of the samples produced after the calcination of  $\text{TiO}_2$  sol using acetylacetone as the hydrolysis control agent (Figure 3 and Supplementary Materials Figure S1), it can be seen that when the calcination temperature was relatively low (100 °C and 300 °C), the particles were large with maximum particle size of 3–5  $\mu\text{m}$  and had poor dispersity. When the calcination temperature increased to 400 and 500 °C, the particle size decreased below 1  $\mu\text{m}$  with good dispersity, which means stable  $\text{TiO}_2$  grains had formed. The grain size increased to 1–2  $\mu\text{m}$  when the calcination temperature was 600 °C. From the TEM image (Figure 3b), it can be seen that its primary grain size was about 20 nm, which was in accordance with the XRD result. The enlarged images showed the interplanar spacing of the (101) face of anatase  $\text{TiO}_2$  to be 0.352 nm. Therefore, the micron size particles in the SEM images are only the aggregates of these nano-sized particles.



**Figure 3.** (a) SEM image of the  $\text{TiO}_2$  powders produced by using acetylacetone as hydrolysis control agent and calcined at 500 °C; (b) TEM image of the  $\text{TiO}_2$  powders produced by using acetylacetone as hydrolysis control agent with calcination temperature 500 °C.

### 3.3. The Optical Properties and Photocatalytic Activity of TiO<sub>2</sub> Obtained by the Calcination of TiO<sub>2</sub> Sol

Figure 4a displays the UV-visible diffuse reflectance spectrum in the wavelength range of 200–800 nm for TiO<sub>2</sub> obtained by the calcination of the TiO<sub>2</sub> sol. Its band-gap value was calculated using the UV-visible absorption spectrum according to the Kubelka–Munk equation [33]:

$$\alpha h\nu = A (h\nu - E_g)^{n/2} \quad (2)$$

where  $\alpha$  is the adsorption coefficient;  $h\nu$  the photo energy;  $A$  the proportionality constant;  $E_g$  the band gap energy (eV).  $n$  equals to 1 or 4, depending on whether the transition is direct or indirect, respectively. Since the transition between the bands in TiO<sub>2</sub> is indirect,  $n = 4$ . The energy of the band gap is calculated by extrapolating a straight line to the abscissa axis. Figure 4b shows the plot of the  $(\alpha h\nu)^{1/2}$  versus  $E_g$ . The band gap of the produced TiO<sub>2</sub> is estimated to be 3.15 eV, which is close to the theoretical band gap (3.2 eV) of anatase TiO<sub>2</sub> powder.

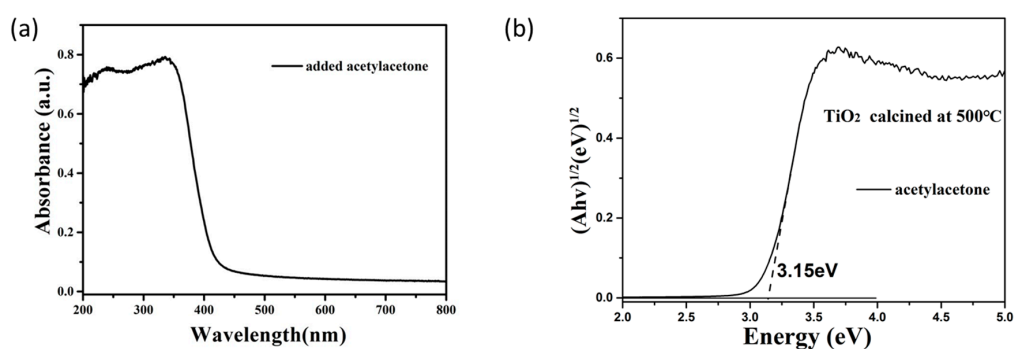


**Figure 4.** (a) UV-vis diffuse reflectance spectrum of TiO<sub>2</sub> produced by using acetylacetonone as the hydrolysis control agent; (b) The plots between  $(\alpha h\nu)^{1/2}$  and  $E_g$  for TiO<sub>2</sub> with acetylacetonone as the hydrolysis control agent.

The photocatalytic performance of the TiO<sub>2</sub> obtained by the calcination of TiO<sub>2</sub> sol was evaluated by decomposition of an aqueous methylene blue solution under UV-light illumination (Figure 5). To achieve the adsorption equilibrium, the solution including methylene blue and the photocatalyst was stirred in dark for 60 min without UV light irradiation. A blank experiment without photocatalyst was also done under the same conditions. The blank experiment shows that during the whole process, the concentration of methylene blue solution remained almost the same, which means that methylene blue was quite stable under illumination.

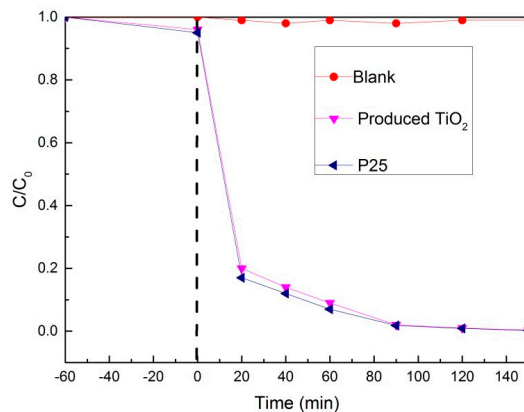


**Figure 5.** Photocatalytic decomposition of methylene blue by the produced TiO<sub>2</sub> using acetylacetonone as the hydrolysis control agent.

From Figure 5, it can be seen clearly that the produced  $\text{TiO}_2$  had an obvious photocatalytic effect. Nearly 90% of the methylene blue was degraded at 40 min and almost all of it was degraded in 90 min. The produced  $\text{TiO}_2$  had similar photocatalytic degradation ability compared with P25. The excellent photocatalytic degradation ability of the produced  $\text{TiO}_2$  will be a great help to the self-cleaning performance of the  $\text{TiO}_2$  film.

### 3.4. The Morphology of $\text{TiO}_2$ Thin Film and Its Self-Cleaning Property

#### 3.4.1. The Morphology of $\text{TiO}_2$ Thin Film

Figure 6 shows the SEM images and Energy Dispersive Spectroscopy (EDS) analysis of the  $\text{TiO}_2$  thin film by using acetylacetone as the hydrolysis control agent at different aging times. The  $\text{TiO}_2$  thin film was quite compact with no aging treatment. As the aging time increased to 6 h and 48 h, a small number of particles with grain size less than 200 nm existed on the  $\text{TiO}_2$  film. The majority of the film was still compact and continuous. The EDS analysis shows that the tiny particles on the surface were  $\text{TiO}_2$ . The results above show that the sol produced using acetylacetone as the hydrolysis control agent can be used to make  $\text{TiO}_2$  thin films.

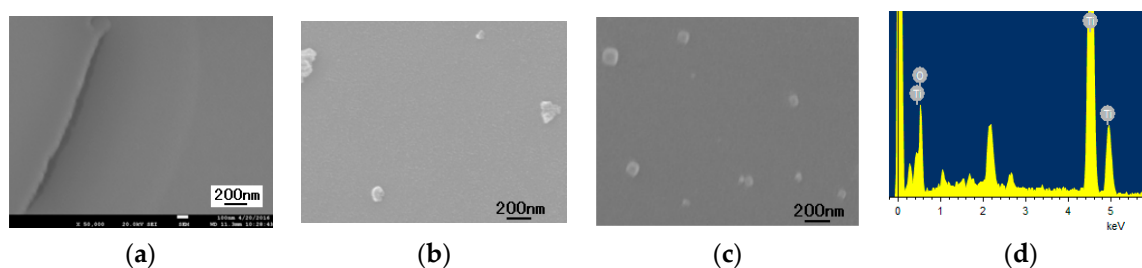


**Figure 6.** SEM images of the  $\text{TiO}_2$  thin film formed using acetylacetone as the hydrolysis control agent (a) aging time 0 h; (b) aging time 6 h; (c) aging time 48 h; (d) The EDS of the thin films.

#### 3.4.2. The Hydrophilicity and Self-Cleaning Property of the $\text{TiO}_2$ Thin Film

Supplementary Materials Figure S2 shows the water contact angles of the  $\text{TiO}_2$  thin films formed by using  $\text{TiO}_2$  sol with acetylacetone as the hydrolysis control agent followed by 30 min ultraviolet illumination. When the calcination temperature was 500 °C, the water contact angle of the thin film was almost 0°, showing an extraordinary light-induced hydrophilic effect and super-hydrophilicity, which may be caused by the large amount of highly crystallized anatase  $\text{TiO}_2$ . The film calcined at 300 °C had a relatively large contact angle because the  $\text{TiO}_2$  formed at this temperature was mostly amorphous and there were still some organic compounds remaining.

The effect of the illumination time to the hydrophilic properties of the film was also investigated. Figure 7 shows water contact angle changes of  $\text{TiO}_2$  film with illumination time. Before illumination, the contact angle of  $\text{TiO}_2$  film was 21°, while after 5 min illumination, the contact angle was reduced to less than 5°, which showed super-hydrophilic properties. The contact angle of  $\text{TiO}_2$  film reduced continuously with illumination time and reached almost 0° when the illumination time was 20 min, which meant complete wetting and super hydrophilicity were realized by then. The above-mentioned light-induced super-hydrophilicity of the  $\text{TiO}_2$  film is an important factor in its self-cleaning ability.

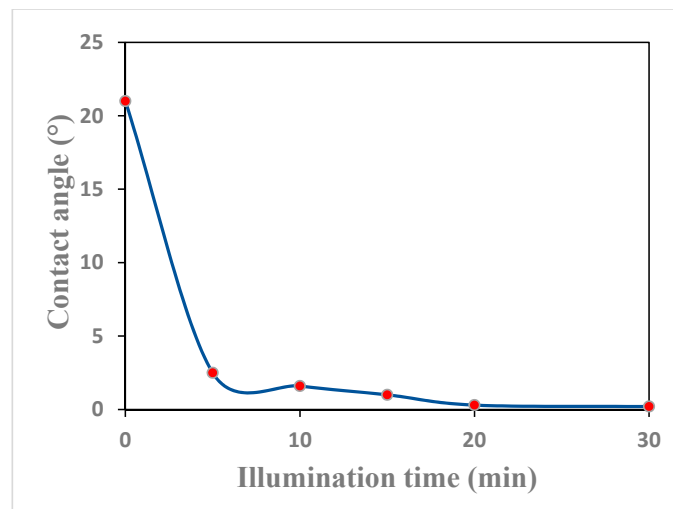


**Figure 7.** Contact angle changes of TiO<sub>2</sub> film with illumination time (Acetylacetone was used as hydrolysis control agent and the calcination temperature was 500 °C).

### 3.4.3. The Antifogging Property of the TiO<sub>2</sub> Thin Film

The self-cleaning function and antifogging property of TiO<sub>2</sub> film were also tested (Figure 8). Methylene blue was used as a kind of organic pollutant to coat the surface of glass slides with or without TiO<sub>2</sub> film. Compared with the glass slide itself, the TiO<sub>2</sub> film before illumination had a relatively smaller water contact angle, therefore, the methylene blue coated on TiO<sub>2</sub> film had a bigger coated area and the coating was more even. After illumination, the glass slides were washed slowly with water. From Figure 8a, it can be seen that the pollutant was still on the glass slides without TiO<sub>2</sub> film coating with an obvious profile, while the glass slides with TiO<sub>2</sub> film regained their cleanness in the center, which meant the TiO<sub>2</sub> film had the self-cleaning function. The antifogging property of TiO<sub>2</sub> film was also tested (Figure 8b). After illumination, the glass slides were sprayed on the surface. A large number of water droplets emerged on the surfaces of glass slides without TiO<sub>2</sub> film, leading to poor vision of the background image. Instead, the glass slides with TiO<sub>2</sub> film were quite clean, which showed the extraordinary antifogging properties as well as the light-induced hydrophilicity of the produced TiO<sub>2</sub> film.

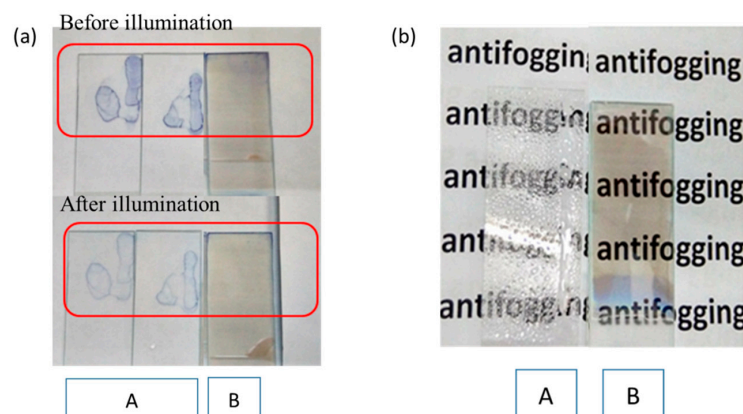


**Figure 8.** (a) The self-cleaning properties of TiO<sub>2</sub> film; (b) The antifogging property of TiO<sub>2</sub> film (A is the glass slides without TiO<sub>2</sub> film; B is the glass slide with TiO<sub>2</sub> film using acetylacetone as the hydrolysis control agent).

#### 4. Conclusions

In this article, we have successfully produced TiO<sub>2</sub> sol by the hydrolysis of tetrabutyl titanate using the sol-gel method. Among the three hydrolysis control agents, acetylacetone is more suitable than triethanolamine and the mixture of acetic acid and hydrochloric acid. When the calcination temperature was 500 °C, the products were in single anatase TiO<sub>2</sub> phase with grain size 18–20 nm. The products after the calcination of the sol at 500 °C had strong absorption of ultraviolet light of wavelengths less than 400 nm and its band gap was calculated as 3.15 eV. It had strong photocatalytic properties and could degrade nearly 100% of methylene blue after 90 min illumination, which is similar to P25. However, it is hard to use P25 to produce TiO<sub>2</sub> thin film compared with the TiO<sub>2</sub> sol used in this research. The final TiO<sub>2</sub> film was compact and continuous and had an obvious light-induced hydrophilic effect and super-hydrophilicity. After 30 min ultraviolet illumination, the contact angle of the obtained TiO<sub>2</sub> film reached almost 0°. It also had a strong anti-fogging capability and excellent self-cleaning ability, making it suitable for products related to our daily lives.

**Supplementary Materials:** The following are available online at [www.mdpi.com/1996-1944/11/3/450/s1](http://www.mdpi.com/1996-1944/11/3/450/s1). Figure S1: SEM images of the TiO<sub>2</sub> powders produced by using acetylacetone as hydrolysis control agent and (a) dried at 100 °C; (b) calcined at 300 °C; (c) calcined at 400 °C; (d) calcined at 600 °C. Figure S2: Contact angle of TiO<sub>2</sub> film by using acetylacetone as the hydrolysis control agent, calcined at different temperatures and ultraviolet irradiated for 30 min.

**Author Contributions:** Yu Liang and Hao Ding conceived and designed the experiments; Yu Liang performed the experiments; Yu Liang, Sijia Sun and Tongrong Deng analyzed the data; Wanting Chen and Ying Chen contributed reagents and materials; Yu Liang wrote the paper.

**Conflicts of Interest:** The authors declare no conflict of interest.

#### References

1. Liang, Y.; Ding, H.; Xue, Q. Characterization of Brucite/TiO<sub>2</sub> Composite Particle Material Prepared by Mechano-Chemical Method. *Surf. Rev. Lett.* **2018**, *25*, 1850085. [[CrossRef](#)]
2. Adachi, M.; Murata, Y.; Takao, J.; Jiu, J.; Sakamoto, M.; Wang, F. Highly efficient dye-sensitized solar cells with a titania thin-film electrode composed of a network structure of single-crystal-like TiO<sub>2</sub> nanowires made by the “oriented attachment” mechanism. *J. Am. Chem. Soc.* **2004**, *126*, 14943–14949. [[CrossRef](#)] [[PubMed](#)]
3. Maeda, K.; Xiong, A.; Yoshinaga, T.; Ikeda, T.; Sakamoto, N.; Hisatomi, T.; Takashima, M.; Lu, D.; Kanehara, M.; Setoyama, T.; et al. Photocatalytic overall water splitting promoted by two different cocatalysts for hydrogen and oxygen evolution under visible light. *Angew. Chem. Int. Ed. Engl.* **2010**, *49*, 4096–4099. [[CrossRef](#)] [[PubMed](#)]
4. Hernandez-Alonso, M.D.; Fresno, F.; Suarez, S.; Coronado, J.M. Development of alternative photocatalysts to TiO<sub>2</sub>: Challenges and opportunities. *Energy Environ. Sci.* **2009**, *2*, 1231–1257. [[CrossRef](#)]
5. Formenti, M.; Juillet, F.; Meriaudeau, P. Heterogeneous photocatalysis for partial oxidation of paraffins. *J. Chem. Technol.* **1971**, *4*, 680–686.
6. Fujishima, A.; Honda, K. Electrochemical photolysis of water at a semiconductor electrode. *Nature* **1972**, *238*, 37–38. [[CrossRef](#)] [[PubMed](#)]
7. Carp, O.; Huisman, C.L.; Reller, A. Photoinduced reactivity of titanium dioxide. *Prog. Solid State Chem.* **2004**, *32*, 133–177. [[CrossRef](#)]
8. Hoffmann, M.R.; Martin, S.T.; Choi, W.; Bahnemann, D.W. Environmental applications of semiconductor photocatalysis. *Chem. Rev.* **1995**, *95*, 69–96. [[CrossRef](#)]
9. Linsebigler, A.L.; Lu, G.Q.; Yates, J.T. Photocatalysis on TiO<sub>2</sub> surfaces: Principles, mechanisms, and selected results. *Chem. Rev.* **1995**, *95*, 735–758. [[CrossRef](#)]
10. Maeda, K.; Domen, K. Photocatalytic Water Splitting: Recent Progress and Future Challenges. *J. Phys. Chem. Lett.* **2010**, *1*, 2655–2661. [[CrossRef](#)]

11. Fujishima, A.; Rao, T.N.; Tryk, D.A. Titanium dioxide photocatalysis. *J. Photochem. Photobiol. C Photochem. Rev.* **2000**, *1*, 1–21. [[CrossRef](#)]
12. Choina, J.; Duwensee, H.; Flechsig, G.-U.; Kosslick, H.; Morawski, A.W.; Tuan, V.A.; Schulz, A. Removal of hazardous pharmaceutical from water by photocatalytic treatment. *Cent. Eur. J. Chem.* **2010**, *8*, 1288–1297. [[CrossRef](#)]
13. Fujishima, A.; Zhang, X.T. Titanium dioxide photocatalysis: Present situation and future approaches. *C. R. Chim.* **2006**, *9*, 750–760. [[CrossRef](#)]
14. Mills, A.; Lee, S.-K. A web-based overview of semiconductor photochemistry-based current commercial applications. *J. Photochem. Photobiol. A Chem.* **2002**, *152*, 233–247. [[CrossRef](#)]
15. Adesina, A.A. Industrial exploitation of photocatalysis: Progress, perspectives and prospects. *Catal. Surv. Asia* **2004**, *8*, 265–273. [[CrossRef](#)]
16. Jalvo, B.; Faraldos, M.; Bahamonde, A.; Rosal, R. Antimicrobial and antibiofilm efficacy of self-cleaning surfaces functionalized by TiO<sub>2</sub> photocatalytic nanoparticles against *Staphylococcus aureus* and *Pseudomonas putida*. *J. Hazard. Mater.* **2017**, *340*, 160–170. [[CrossRef](#)] [[PubMed](#)]
17. Tan, B.Y.L.; Tai, M.H.; Juay, J.; Liu, Z.; Sun, D. A study on the performance of self-cleaning oil–water separation membrane formed by various TiO<sub>2</sub> nanostructures. *Sep. Purif. Technol.* **2015**, *156*, 942–951. [[CrossRef](#)]
18. Kormann, C.; Bahnemann, D.W.; Hoffmann, M.R. Photolysis of Chloroform and Other Organic Molecules in Aqueous TiO<sub>2</sub> Suspensions. *Environ. Sci. Technol.* **1991**, *25*, 494–500. [[CrossRef](#)]
19. Thampi, K.R.; Reddy, T.V.; Ramakrishnan, V.; Kuriacose, J.C. Mechanism of photoelectrocatalytic dehydrogenation of 2-propanol on a polycrystalline ZnO Photoelectrode. *Electrochim. Acta* **1983**, *28*, 1869–1874. [[CrossRef](#)]
20. Kandavelu, V.; Kastien, H.; Thampi, K.R. Photocatalytic degradation of isothiazolin-3-ones in water and emulsion paints containing nanocrystalline TiO<sub>2</sub> and ZnO catalysts. *Appl. Catal. B Environ.* **2004**, *48*, 101–111. [[CrossRef](#)]
21. Ge, L.; Liu, J. Efficient visible light-induced photocatalytic degradation of methyl orange by QDs sensitized CdS-Bi<sub>2</sub>WO<sub>6</sub>. *Appl. Catal. B Environ.* **2011**, *105*, 289–297. [[CrossRef](#)]
22. Ganesh, V.A.; Raut, H.K.; Nair, A.S.; Ramakrishna, S. A review on self-cleaning coatings. *J. Mater. Chem.* **2011**, *21*, 16304–16322. [[CrossRef](#)]
23. Kim, S.M.; In, I.; Park, S.Y. Study of photo-induced hydrophilicity and self-cleaning property of glass surfaces immobilized with TiO<sub>2</sub> nanoparticles using catechol chemistry. *Surf. Coat. Technol.* **2016**, *294*, 75–82. [[CrossRef](#)]
24. Petica, A.; Gaidau, C.; Ignat, M.; Sendrea, C.; Anicai, L. Doped TiO nanophotocatalysts for leather surface finishing with self-cleaning properties. *J. Coat. Technol. Res.* **2015**, *12*, 1–11. [[CrossRef](#)]
25. Lucas, S.S.; Barroso de Aguiar, J.L. Multifunctional wall coating combining photocatalysis, self-cleaning and latent heat storage. *Mater. Res. Express* **2018**, *5*, 025702. [[CrossRef](#)]
26. Zhang, L.; Wang, Y.; Yu, R. Research on photocatalytic self-cleaning of pure cotton fabric coated with nano TiO<sub>2</sub>. *Shanghai Text. Sci. Technol.* **2015**, *43*, 54–56.
27. Suyama, Y.; Kato, A. TiO<sub>2</sub> Produced by Vapor-Phase Oxygenolysis of TiCl<sub>4</sub>. *J. Am. Ceram. Soc.* **1976**, *59*, 146–149. [[CrossRef](#)]
28. Valletregi, M.; Ragel, V.; Roman, J.; Martinez, J.L.; Labeau, M.; Gonzalezcalbet, J.M. Texture evolution of SnO<sub>2</sub> synthesized by pyrolysis of an aerosol. *J. Mater. Res.* **1993**, *8*, 138–144. [[CrossRef](#)]
29. Chen, J.; Dong, X.; Xin, Y.; Zhao, M. Effects of titanium dioxide nano-particles on growth and some histological parameters of zebrafish (*Danio rerio*) after a long-term exposure. *Aquat. Toxicol.* **2011**, *101*, 493. [[CrossRef](#)] [[PubMed](#)]
30. Wang, H.; Wick, R.L.; Xing, B. Toxicity of nanoparticulate and bulk ZnO, Al<sub>2</sub>O<sub>3</sub> and TiO<sub>2</sub> to the nematode *Caenorhabditis elegans*. *Environ. Pollut.* **2009**, *157*, 1171–1177. [[CrossRef](#)] [[PubMed](#)]
31. Barbana, N.; Ben Youssef, A.; Dhiflaoui, H.; Bousselmi, L. Preparation and characterization of photocatalytic TiO<sub>2</sub> films on functionalized stainless steel. *J. Mater. Sci.* **2018**, *53*, 3341–3363. [[CrossRef](#)]

32. Liu, J.; Zhao, H.; Song, X.; Li, X. Effects of calcination temperature on structure of titanium dioxide photocatalyst. *Inorg. Chem. Ind.* **2009**, *41*, 37–39.
33. Sang, Y.; Zhao, Z.; Zhao, M.; Hao, P.; Leng, Y.; Liu, H. From UV to Near-Infrared, WS<sub>2</sub> Nanosheet: A Novel Photocatalyst for Full Solar Light Spectrum Photodegradation. *Adv. Mater.* **2015**, *27*, 363–369. [[CrossRef](#)] [[PubMed](#)]



© 2018 by the authors. Licensee MDPI, Basel, Switzerland. This article is an open access article distributed under the terms and conditions of the Creative Commons Attribution (CC BY) license (<http://creativecommons.org/licenses/by/4.0/>).